Journal of Science and Transport Technology
Journal homepage: https://jstt.vn/index.php/en

Comparison of essential physical properties between pristine armchair silicene nanoribbons and those doped with Ge and As

Dang Phuc Kien Cuong[1], Tran Minh Tien[2,*]
[1]Nam Ky Khoi Nghia high school, Tien Giang Province, Vietnam; email: cuongtg1984@gmail.com
[2]Thu Dau Mot University, Binh Duong Province, Vietnam; email: tientm@tdmu.edu.vn

Article info
Type of article:
Original research paper

DOI:
https://doi.org/10.58845/jstt.utt.2024.en.4.4.110-118

***Corresponding author:**
Email address:
tientm@tdmu.edu.vn

Received: 14/11/2024
Revised: 20/12/2024
Accepted: 23/12/2024

Abstract: In this paper, some physical properties of pristine armchair silicene nanoribbons (ASiNR) and those doped with Ge (ASiGeNR) and As (ASiAsNR) using the VASP (Vienna ab initio simulation package) computational program, by using density functional theory. The results show significant differences in the structural and electronic properties between these systems. For ASiGeNR and ASiAsNR, structural parameters such as the distance between two nearest-neighbor atoms in the hexagonal ring, the distance between two farthest atoms, and the buckling height are all larger compared to ASiNR. While ASiNR and ASiGeNR have band gaps of approximately 0.262 eV and 0.2410 eV, respectively, opening at the Γ point, ASiAsNR does not have a band gap. The results indicate that ASiNR and ASiGeNR exhibit semiconductor properties, while ASiAsNR exhibits metallic properties. For ASiGeNR, the substitution of Ge leads to a reduction in bandgap and an increase in thermal conductivity, attributed to the energy level of Ge being close to that of Si. For ASiAsNR, the substitution with As increases the density of states at the top of the valence band, suggesting better electrical conductivity. ASiNR, with its wide bandgap, is suitable for applications in semiconductor devices such as MOSFETs and sensors. ASiGeNR is well-suited for optoelectronic applications such as solar cells or light-emitting diodes (LEDs), while ASiAsNR is appropriate for spintronics or high-speed electronic devices.
Keywords: VASP, armchair SiNR, doped, electronic properties.

1. Introduction

Silicene is a material with great potential applications in the field of electronics. Since silicene is based on silicon atoms, which are fundamental in current electronic devices, integrating silicene would be more advantageous compared to materials based on other atoms. Silicene has a honeycomb structure similar to graphene, but its surface has a certain degree of buckling and is not as flat as graphene. However, a significant limitation of 2D silicene is that its band gap is nearly zero, which greatly restricts its applications in electronic devices. Researchers have explored various methods to introduce a band gap, including applying an electric field, employing chemical techniques, creating structural defects, or adsorbing atoms onto the surface.

In 2011 a study showed that the band gap of

silicene and germanene increases linearly with the longitudinal electric field strength, The band gap size and effective mass of charge carriers increase linearly with the electric field strength [1]. Chemical techniques, such as hydrogenation or halogenation, have also been applied to introduce a band gap in silicene [2-4]. The core properties of 2D silicene influenced by the adsorption of B, N, Al, and P atoms on its surface have been studied [5-9]. Studies have also shown that adsorption of certain metals such as alkali metals, sickle earth metals, and transition metals also leads to different results. Research has shown that Li favors "hollow" or "valley" adsorption sites on silicene, while most alkaline earth metals (except Ca) prefer the "valley" sites. However, Ca adsorption can disturb the silicene structure. Structural stability of edge-hydrogenated and edge-fluorinated SiNRs has been evaluated [10].

The structural and electronic properties of silicene combined with various other atoms have also been studied [11-14]. The results show that armchair SiC nanoribbons are non-magnetic semiconductors, while zigzag SiC nanoribbons are magnetic metals. Zigzag SiC nanoribbons with widths of 2-4 atoms exhibit metallic properties with a small band gap. For armchair SiC nanoribbons, the p-orbitals of C and Si mainly contribute around the Fermi level, and the band gap of armchair SiC is larger compared to zigzag SiC nanoribbons. Recently, nanoribbon systems based on the combination of Si and Ge, called Siligene, have attracted significant attention due to their wide application potential in sensors and nanoelectronics [15-17]. HSiGe is a magnetic semiconductor with a bandgap of approximately 0.6 eV. The electronic properties of SiGe and its derivatives can be tuned by applying mechanical strain and external electric fields. SiGe structures and their derivatives hold great potential for applications in nano-scale electronic devices. The results also show that 2D SiGe remains dynamically stable under tensile strains of 4% and 6%. A band inversion at the Γ point is observed with a bandgap of 25 meV for 6% strain due to spin-orbit coupling (SOC). SiGe nanoribbons with edge states exhibit valence and conduction bands crossing at the Γ point to form a Dirac cone, topologically protected within the bandgap. The findings further indicate that 2D SiGe is thermally and dynamically stable, with negative formation energy and no imaginary frequencies in its phonon spectrum. SiGe offers low diffusion energy barriers for alkali metal atoms (0.14–0.35 eV), enabling fast charge/discharge rates. The SiGe layer has a high theoretical capacity (1064 mAh/g for Na and 532 mAh/g for K) and stable voltage profiles. Alkali metal atoms adsorbed on the SiGe layer enhance its electrical conductivity, making it suitable for various advanced applications.

Several nanoribbon structures formed by atoms have garnered research interest. The ZSiCNRs are metallic except for thinner ribbons (Nz = 2-4) with small direct band gaps. ASiCNRs exhibit sawtooth-like periodic oscillation features in their direct band gaps, which quench to a constant value of 2.359 eV as the width increases. The charge density contours show significant electron transfer from Si atoms to C atoms, indicating an ionic binding feature. The Si-H bond is ionic, while the C-H bond is covalent [18]. Quasiparticle band gaps are significantly increased by up to 2 eV compared to Kohn-Sham energy values; inclusion of electron-hole interactions modifies the absorption spectra, resulting in strongly bound excitonic peaks and Hydrogen-passivated SiC nanoribbons are more stable than bare ones, making them suitable for optoelectronic devices [19]. Perfect ZSiGeNRs are weak magnetic semiconductors. ZSiGeNRs with bare Si or Ge edges are weak magnetic metals, and those with bare Si and Ge edges are nonmagnetic metals; the charge density contours show significant electron transfer from Si or Ge atoms to H atoms, indicating an ionic binding feature [20]. The nanoribbon synthesis proceeds faster than the diffusion of Si to

the Ge surface, and threading dislocations in the Ge epilayer do not affect the nucleation or anisotropic growth kinetics of the nanoribbons; these results suggest that previous successes in graphene nanoribbon synthesis on Ge(001) can be extended to Si(001) by using epilayers of Ge, motivating future exploration of this platform for hybrid semiconducting graphene/Si electronics [21]. The armchair SnGe and SnC nanoribbons are direct semiconductors with band gaps that converge to 1.71 eV for A-SnCNRs and 0.15 eV for A-SnGeNRs as the width increases; A-SnCNRs show no absorption in the lower energy range (0 to 1.2 eV), while A-SnGeNRs exhibit absorption in the near-infrared to visible spectrum [22]. All studied SiX monolayers are semiconductors with moderate band gaps, except for SiBi, which is a direct bandgap semiconductor; carrier mobility calculations indicate p-type semiconducting nature for SiN, SiP, and SiBi, and n-type for SiAs and SiSb; the findings suggest that these SiX monolayers are promising candidates for thermoelectric materials at room temperature, with potential applications in microelectronic and thermoelectric devices [23].

In this paper, some essential physical properties between pristine armchair silicene nanoribbons (ASiNR) and those doped with Ge (ASiGeNR) and As (ASiAsNR) are examined in detail. This will provide specific evaluations of the application potential of these material structures in practical fields.

2. Methodology

The structures of the systems are constructed as follows: unit cell of ASiAsNR and ASiGeNR has 16 atoms (Si, As/Ge, H). On either side of each structure is functionalized by hydrogen atoms to increase sustainability. To enhance structural stability, the edges of these structures are passivated. Fig 1 illustrates the unit cells of these systems. Using density functional theory (DFT) calculations with the Vienna ab initio simulation package (VASP) [24, 25], we investigate the electronic and atomic structures of these systems. The generalized quasi-gradient method is used to calculate the exchange correlation energy of electrons [26], with PBE (Perdew–Burke–Ernzerhof) and PAW (Projector-Augmented Wave) functions [27]. The energy cutoff is set at 500 eV. The kpoints wave vector is set to 1x1x8 for the optimal atomic positioning calculations and 1x1x32 for the self-consistent calculations.

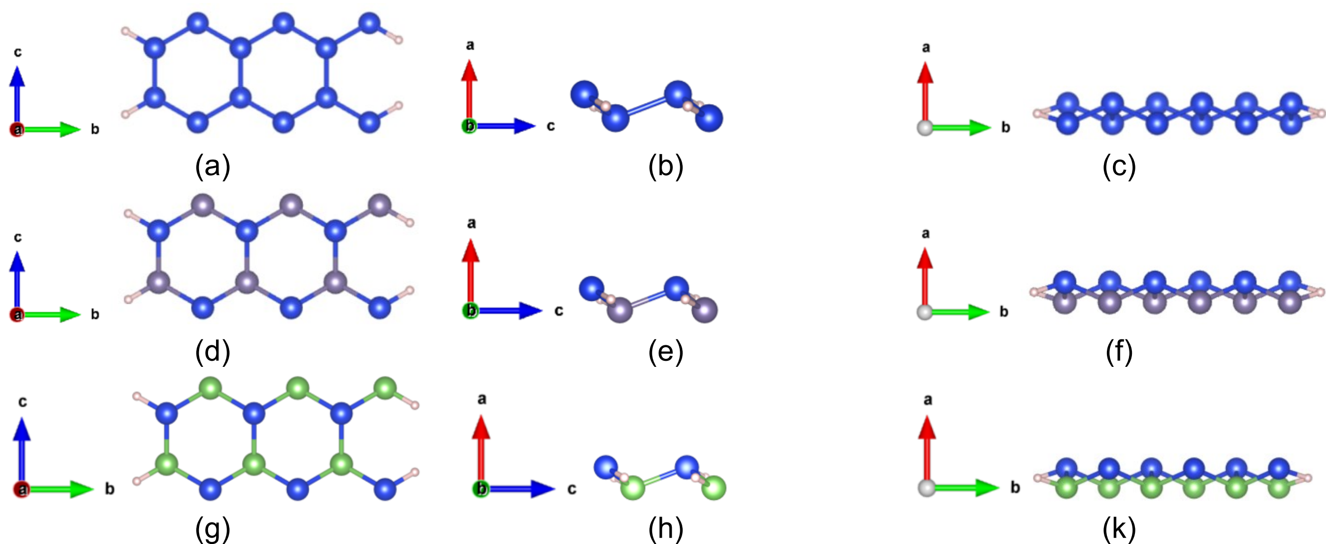

Fig 1. Optimized Structures of ASiNR, ASiGeNR, and ASiAsNR
(a, b, c) Structures of ASiNR from different directions
(d, e, f) Structures of ASiGeNR from different directions
(g, h, k) Structures of ASiAsNR from different directions

The optimization process stops when the force is less than 0.01 eVÅ^{-1}; the convergence energy is set to 10^{-5} eV between the two nearest ion steps. After the optimization process, the calculation of the single point is carried out; for calculating and comparison the essential physical properties of these systems.

3. Results and Discussion

3.1. Structure after optimization

After the structural optimization calculations, the positions of the atoms are determined. Table 1 presents the basic parameters of the optimized structures such as the first and second distances between two atoms and the buckling of the structure. Here, the first and second distances are determined from the first Si atom to the 2 neighboring atoms in the hexagonal ring.

The results show significant structural differences between the configurations. The first distance of ASiNR differs by 0.06664 Å and 0.12720 Å compared to ASiGeNR and ASiAsNR, respectively. This indicates that the shortest distance between two atoms in the hexagonal ring increases when doped with Ge and As; this increase is relatively small in the case of Ge but quite significant with As. The second distance changes similarly, with differences between ASiNR and the two doped structures being 0.06923 Å and 0.21347 Å, respectively. The differences between the first and second distances in the structures also vary. For ASiNR, Δr = 0.04830 Å; for ASiGeNR and ASiAsNR, the Δr values are 0.05089 Å and 0.13457 Å, respectively. The buckling of the structure also shows considerable differences between ASiNR, ASiGeNR, and ASiAsNR. For ASiNR, the buckling is 0.55758 Å, while for ASiGeNR and ASiAsNR, it is 0.79966 Å and 1.74860 Å, respectively. These differences arise from the variations in bonding forces between Si-Si, Si-Ge, and Si-As atoms, as well as charge distribution. This will be further clarified in the following sections.

Table 1. Structural parameters

Structure	First Distance r_1 (Å)	Second Distance r_2(Å)	$\Delta r=r_1-r_2$ (Å)	Buckling δ(Å)
ASiNR	2.20991	2.25821	0.04830	0.55758
ASiGeNR	2.27655	2.32744	0.05089	0.79966
ASiAsNR	2.33711	2.47168	0.13457	1.74860

3.2. The electronic band structure

The fundamental electronic properties, allowing for the evaluation of whether the material system behaves as a semiconductor or a metal will be evaluated based on the electronic band structure. The Fig 2 presents the electronic band structures for three armchair nanoribbon systems: ASiNR (2a), ASiGeNR (2b), and ASiAsNR (2c). These results reveal important information about their electronic properties, orbital contributions, and band gaps. With ASiNR, a band gap of approximately 0.26 eV is observed at the Γ point, indicating semiconductor behavior; the contributions from Si-3px and Si-3py orbitals dominate around the Fermi level; Si-3pz orbitals primarily contribute below the Fermi level, while Si-3s orbitals are concentrated in the valence band region; the band structure shows well-defined conduction and valence bands, with limited dispersion near E_F, consistent with the semiconductor nature. With ASiGeNR, a direct band gap of approximately 0.2410 eV at the Γ point indicates that ASiGeNR also exhibits semiconductor properties. Both Si and Ge contribute significantly to the bands near E_F, with Ge having a more prominent role than Si. H contributions are negligible and appear deep below the valence band. The orbital analysis reveals that the s, px, py, and pz orbitals of Si and Ge provide similar contributions to the band structure. Si-3px

and Ge-4px orbitals are dominant around E_F, while Si-3py, Si-3pz, Ge-4py, and Ge-4pz contribute more below E_F. The band structure exhibits slightly less symmetry than ASiNR, reflecting the influence of Ge atoms and their bonding characteristics. With AsiAsNR. The band structure demonstrates a metallic behavior, with energy levels crossing E_F from the valence to the conduction band; contributions from Si and As dominate near E_F, with Si having a greater impact closer to E_F and As dominating below it. H's contribution remains negligible throughout; the s orbitals of Si and As mainly contribute to the conduction band, while px, py, and pz orbitals dominate the regions near and below E_F. Overlaps between the s and px-py orbitals of Si and As suggest possible sp2 and sp3 hybridization in this structure.

These results show that ASiNR and ASiGeNR are semiconductors with small band gaps, while ASiAsNR displays metallic behavior with no band gap. In ASiNR, contributions are exclusively from Si orbitals, while ASiGeNR involves significant Ge participation alongside Si. In ASiAsNR, both Si and As contribute prominently, with a slight dominance of Si near E_F. Both ASiGeNR and ASiAsNR show signs of potential sp2 and sp3 hybridization due to orbital overlaps, whereas ASiNR exhibits more localized bonding characteristics. ASiNR has a simpler, more symmetrical band structure due to uniform Si bonding. In contrast, ASiGeNR and ASiAsNR exhibit more complex band structures due to the inclusion of Ge and As atoms, which alter bonding and orbital interactions. These distinctions highlight the impact of atomic composition on the electronic and orbital properties of these nanoribbons, making them suitable for different applications depending on their behavior (e.g., semiconductor or metallic).

3.3. The electronic density of state (DOS) distributions

Investigating the DOS will further clarify the electronic properties. Fig 3 presents the DOS for the ASiNR (3a), ASiGeNR (3b), and ASiAsNR (3c) structures.

The findings show that ASiNR lacks electronic states near the Fermi energy level. This indicates that there are the presence of a band gap in these structures. The positions of the peaks indicate that Si-3px3py orbitals dominate the density of states compared to other orbitals, highlighting their major contribution, particularly just below and above the Fermi level. In these regions, the overlapping peaks from Si-3px3py and Si-3pz orbitals suggest potential mixed sp2 and sp3 orbital overlap. Additionally, the energy peaks also show that the DOS from Si3s orbitals appear at high level in the lower valence region, show that these orbitals main contribution to that area. For ASiGeNR structure, the results also indicate that around the Fermi level, the electronic density of states is zero, which reaffirms the presence of a band gap around this level. The DOS is primarily maximum around -2 eV and 2 eV, with significant contributions from Si and Ge; Ge contributes more than Si at most energy levels. The results also show that the contributions from Si-3s and Ge-4s orbitals are mainly in the valence region, around -8 eV, while the p_x, p_y, p_z orbitals are most prominent around the Fermi level. Additionally, there is the sp^2 and sp^3 hybridization in the ASiGeNR structure. For the ASiAsNR structure, the results show that metallic behavior is evident, as the DOS crosses E_F, indicating that conduction occurs without a band gap. Si has significant contributions near E_F, especially in the conduction band, highlighting its primary role in metallic properties; As contributes predominantly in the deeper valence regions (-6 to -3 eV), with a smaller role near E_F compared to Si. H contributions remain negligible, similar to ASiGeNR, concentrated only in the deep valence region. Overlapping contributions between Si and As suggest strong hybridization, particularly evident in the peaks below E_F.

So, in ASiNR, Si orbitals alone define the DOS, while in ASiGeNR and ASiAsNR, the

additional Ge and As atoms introduce more states, enhancing hybridization; ASiGeNR has a more complex DOS profile, reflecting strong bonding and hybridization between Si and Ge; ASiAsNR shows overlapping contributions from Si and As, consistent with sp2/sp3 hybridization, leading to metallic conductivity. These results highlight the effects of atomic substitution on the electronic properties of armchair nanoribbons, offering insight into their potential applications in electronic and optoelectronic devices.

3.4. Charge density distribution

The Fig 4 illustrates the charge density distribution of three armchair nanoribbon structures: ASiNR (a), ASiGeNR (b), and ASiAsNR (c). The charge density distribution shows the bond strength and physical properties within these structures. In the ASiNR system (a), the charge density is strongly concentrated between the silicon atoms, indicating robust covalent bonds with low polarity. In ASiGeNR (b), the charge density between silicon and germanium atoms is slightly reduced compared to ASiNR, reflecting a weakening of the bonds due to the difference in electronegativity between Si and Ge. This leads to more polar bonds, though they retain covalent character. For ASiAsNR (c), the charge density becomes more localized, with significantly reduced density in certain regions, particularly around the arsenic atoms. This indicates that Si-As bonds are weaker and exhibit pronounced polarity, potentially affecting the overall stability of the system. The results indicate that for ASiNR, the sigma bonding made by Si-3s orbitals and Si-3px, Si-3p$_y$ orbitals is larger than the pi-bonding, made by Si-3pz orbitals.

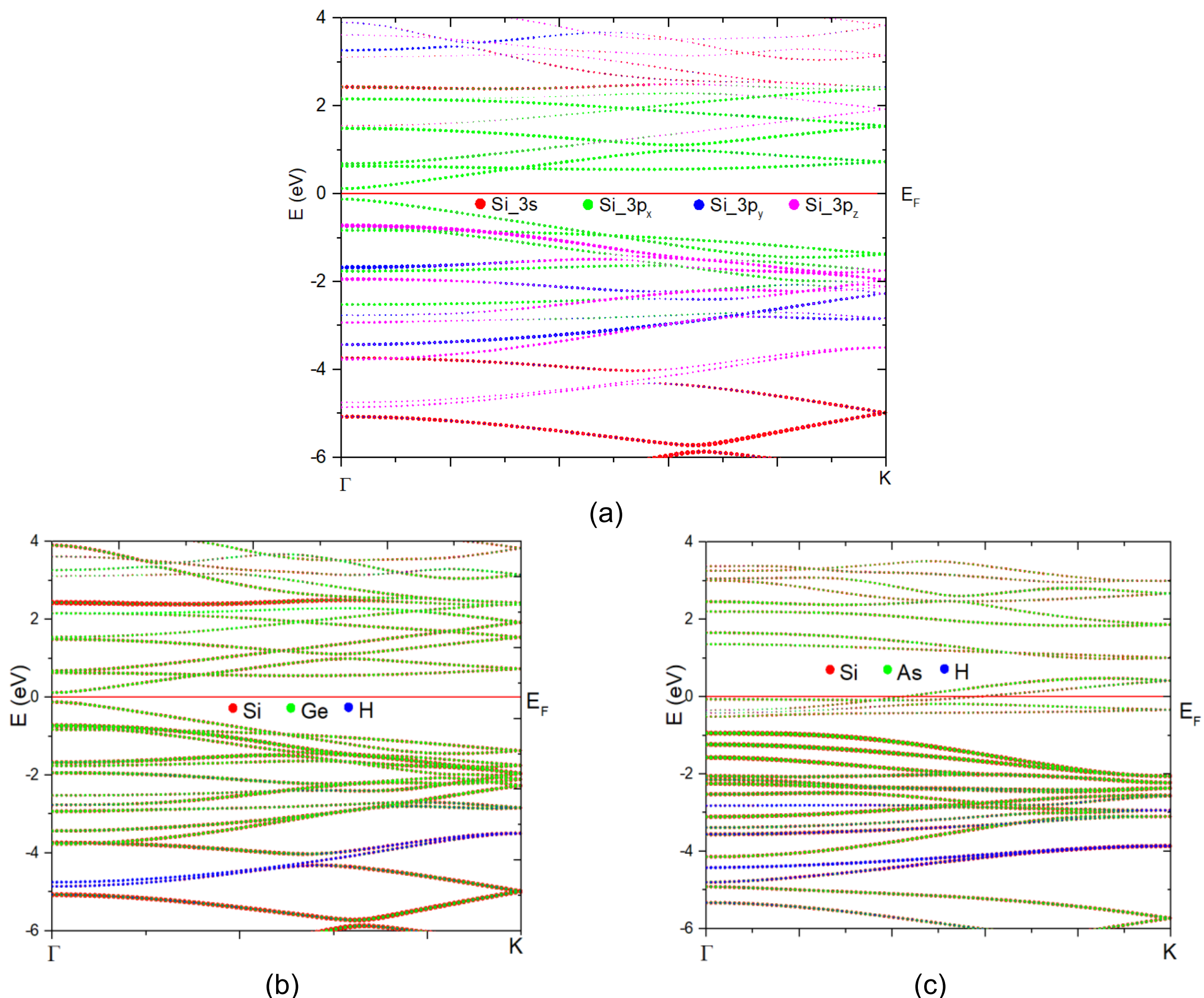

Fig 2. Electronic band structure of ASiNR (a), ASiGeNR (b) and ASiAsNR (c)

(a)

(b) (c)

Fig 3. Electronic state density of ASiNR (a), ASiGeNR (b) and ASiAsNR (c) systems

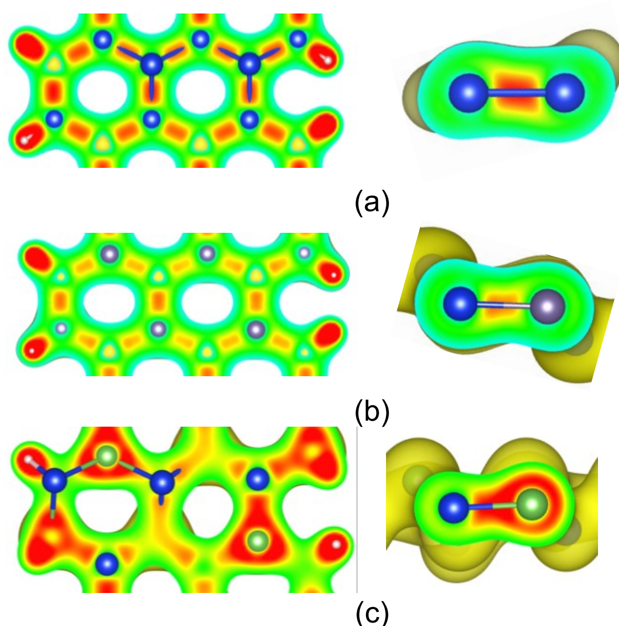

(a)

(b)

(c)

Fig 4. Charge density distribution of ASiNR (a), ASiGeNR (b) and ASiAsNR (c) systems

For the ASiGeNR structure, the σ-bonding strength of Si-3s, Si-3px, Si-3py, Ge-4s, Ge-4px, and Ge-4py orbitals is relatively stronger than the π-bonding of Si-3pz and Ge-4pz orbitals. The results also indicate that the σ-bonding between adjacent Si-Ge atoms is more pronounced compared to the bonding between Si-Ge atoms that are farther apart. For the ASiAsNR structure, the results similarly show that the σ-bonding strength of Si-3s, Si-3px, Si-3py, As-4s, As-4px, and As-4py orbitals is relatively stronger than the π-bonding of Si-3pz and As-4pz orbitals. The results also demonstrate that the σ-bonding between adjacent Si-As atoms is more distinct compared to the bonding between Si-As atoms that are farther apart. Overall, the variations in charge density distribution reveal changes in bonding characteristics as the atomic composition of the nanoribbon systems is altered. ASiNR exhibits the strongest bonds, while ASiGeNR and ASiAsNR display weaker bonds due to increased polarity. These differences may influence the stability and electronic properties of the respective systems.

4. Conclusion

The paper presents research findings comparing certain structural and electronic characteristics of pristine armchair silicene nanoribbons (ASiNR) and those doped with Ge and As. The main results achieved in this study are:

1/ Construction and optimization of the structures of ASiNR, ASiGeNR, and ASiAsNR systems.

2/ Identification of structural changes before and after doping with Ge and As.

3/ Determination of electronic properties through the analysis of electronic band structures and density of states, along with a comparison of the electronic characteristics among the systems, including the contributions of atoms and orbitals to the band structures.

The results show that ASiNR, ASiGeNR, and ASiAsNR structures have great potential for use in various fields, semiconductor devices, sensors optoelectronic, solar cells or light-emitting diodes (LEDs), spintronics or high-speed electronic devices; however, more detailed research is needed.

Acknowledgments

This study uses the resources of the high-performance computing cluster (HPCC) at Thu Dau Mot University.

References

[1] Z. Ni, Q. Liu, K. Tang, J. Zheng, J. Zhou, R. Qin, Z. Gao, D. Yu, J. Lu. (2012). Tunable Bandgap in Silicene and Germanene. *Nano letters*, 12(1), 113-118.

[2] J. Zhao et al. (2016). Rise of silicene: A competitive 2D material. *Progress in Materials Science*, 83, 24-151.

[3] M. Houssa, E. Scalise, K. Sankaran, G. Pourtois, V.V. Afanas'ev, A. Stesmans. (2011). Electronic properties of hydrogenated silicene and germanene. *Applied Physics Letters*, 98(22), 223107.

[4] N. Gao, W.T. Zheng, and Q. Jiang. (2012). Density functional theory calculations for two-dimensional silicene with halogen functionalization. *Physical Chemistry Chemical Physics*, 14(1), 257-261.

[5] J. Sivek, H. Sahin, B. Partoens, F.M. Peeters. (2013). Adsorption and absorption of boron, nitrogen, aluminum, and phosphorus on silicene: Stability and electronic and phonon properties. *Physical Review B*, *87*(8), 085444.

[6] T.P. Kaloni, U. Schwingenschlögl. (2014). Effects of heavy metal adsorption on silicene. *physica status solidi (RRL)- Rapid Research Letters*, 8(8), 685-687.

[7] H. Liu, N. Han, and J. Zhao. (2014). Band gap opening in bilayer silicene by alkali metal intercalation. *Journal of Physics: Condensed Matter*, 26(47), 475303.

[8] R. Quhe et al. (2012). Tunable and sizable band gap in silicene by surface adsorption. *Scientific Reports*, 2, 853.

[9] H. Sahin and F.M. Peeters. (2013). Adsorption

of alkali, alkaline-earth, and 3d transition metal atoms on silicene. *Physical Review B*, 87, 085423.

[10] S.M. Aghaei, I. Torres, I. Calizo. (2016). Structural stability of functionalized silicene nanoribbons with normal, reconstructed, and hybrid edges. *Journal of Nanomaterials*, 2016, 5959162.

[11] S. Lian et al. (2008). Electronic structures of SiC nanoribbons. *The Journal of Chemical Physics*, 129(17), 174114.

[12] J.-M. Zhang et al. (2010). First-principles study on electronic properties of SiC nanoribbon. *Journal of Materials Science*, 45, 3259-3265.

[13] H.A. Badehian, Z. Badehian, R. Sharifirad. (2021). Structural and Electronic Properties of Armchair Silicon Carbide Nanoribbon. *Current Applied Sciences*, 1(1), 51-58.

[14] P. Lou, and J.Y. Lee. (2009). Band structures of narrow zigzag silicon carbon nanoribbons. *The Journal of Physical Chemistry C,* 113(29), 12637-12640.

[15] P. Jamdagni et al. (2015). Stability and electronic properties of SiGe-based 2D layered structures. *Materials Research Express*, 2(1), 016301.

[16] T. Teshome, and A. Datta. (2018). Topological insulator in two-dimensional SiGe induced by biaxial tensile strain. *ACS Omega,* 3(1), 1-7.

[17] A. Sannyal, Y. Ahn, J. Jang. (2019). First-principles study on the two-dimensional siligene (2D SiGe) as an anode material of an alkali metal ion battery. *Computational Materials Science*, 165, 121-128.

[18] J.-M. Zhang, F.L. Zheng, Y. Zhang, V. Ji. (2010). First-principles study on electronic properties of SiC nanoribbon. *Journal of Materials Science*, 45, 3259-3265.

[19] N. Alaal, V. Loganathan, N. Medhekar, A. Shukla. (2016). First principles many-body calculations of electronic structure and optical properties of SiC nanoribbons. *Journal of Physics D: Applied Physics*, 49(10), 105306.

[20] J.-M. Zhang, W.-T. Song, J. Zhang, K.-W. Xu. (2014). Dangling bond modulating the electronic and magnetic properties of zigzag SiGe nanoribbon. *Physica E: Low-dimensional Systems and Nanostructures*, 58, 1-5.

[21] V. Saraswat et al. (2019). Synthesis of armchair graphene nanoribbons on germanium-on-silicon. *The Journal of Physical Chemistry C*, 123(30), 18445-18454.

[22] S. Damizadeh, M. Nayeri, F.K. Fotooh, S. Fotoohi. (2020). Electronic and Optical Properties of SnGe and SnC Nanoribbons: A First-Principles Study. *Journal of Optoelectronical Nanostructures*, 5(4), 67-86.

[23] R.N. Somaiya, Y.A. Sonvane, S.K. Gupta. (2020). Exploration of the strain and thermoelectric properties of hexagonal SiX (X= N, P, As, Sb, and Bi) monolayers. *Physical Chemistry Chemical Physics*, 22(7), 3990-3998.

[24] G. Kresse, J. Furthmüller. (1996). Efficiency of ab-initio total energy calculations for metals and semiconductors using a plane-wave basis set. *Computational Materials Science*, 6(1), 15-50.

[25] G. Kresse, J. Furthmüller. (1996). Efficient iterative schemes for ab initio total-energy calculations using a plane-wave basis set. *Physical Review B*, 54(16), 11169-11186.

[26] J.P. Perdew, K. Burke, M. Ernzerhof. (1996). Generalized gradient approximation made simple. *Physical Review Letters*, 77(18), 3865-3868.

[27] G. Kresse, D. Joubert. (1999). From ultrasoft pseudopotentials to the projector augmented-wave method. *Physical Review B*, 59(3), 1758-1775.